aided by the development of complete software packages to deal with all aspects of data collection and handling. Earlier program packages (Howard, Nielson & Xuong, 1985; Pflugrath & Messerschmidt, 1987; Thomas, 1987) tended to be specific to one particular detector and its associated diffractometer. However, following the initiative of Bricogne (1987) and with financial assistance from EEC funds, a group of scientists, including most of the originators of the earlier packages, are now collaborating in writing, extending, and maintaining a comprehensive device-independent position-sensitive-detector software package.

Acknowledgements

Many helpful comments on this article by Drs A. R. Faruqi, H. E. Schwarz, and D. J. Thomas are gratefully acknowledged.

7.1.7. X-ray-sensitive TV cameras (By J. Chikawa)

High-resolution X-ray imaging systems are required for the topographic study of spatial change in crystal structures, such as that which takes place in phase transformations. From this point of view, high-resolution TV camera tubes will be described.

7.1.7.1. *Signal-to-noise ratio*

Video displays of X-ray and optical images have different features. Although X-ray photon energies are very large, the intensities available in X-ray diffraction are extremely low compared with optical images. Therefore, the photon noise resulting from the statistical fluctuation of the number of photons incident upon an image system gives a detection limit of the image.

Consider the case of defects in a crystal viewed by an imaging system: ν_p photons s^{-1} mm^{-2} are diffracted from the perfect region of a crystal, and $q\nu_p$ ($q < 1$) are absorbed by the X-ray-sensing layer of the system. An absorbed photon produces a mean number η_1 of electrons or visible photons, each of which may be rescattered to produce a mean number η_2 of electrons or photons. By repeating s such processes, the mean signal height

$$S_p = q\nu_p\eta_1\eta_2 \ldots \eta_s\delta^2 t \qquad (7.1.7.1)$$

is obtained from each square-shaped picture element $\delta \times \delta$ mm for t s. The value of δ may be taken as the limiting resolution of the system. Since $\eta_1 > 100$ owing to the large photon energy and the values of $\eta_2, \eta_3, \ldots, \eta_s$ are considered to be less than 100, the photon noise σ_p as a standard deviation of S_p is given by (Arcese, 1964)

$$\sigma_p = \eta_s\eta_{s-1} \ldots \eta_1(q\nu_p\delta^2 t)^{1/2}. \qquad (7.1.7.2)$$

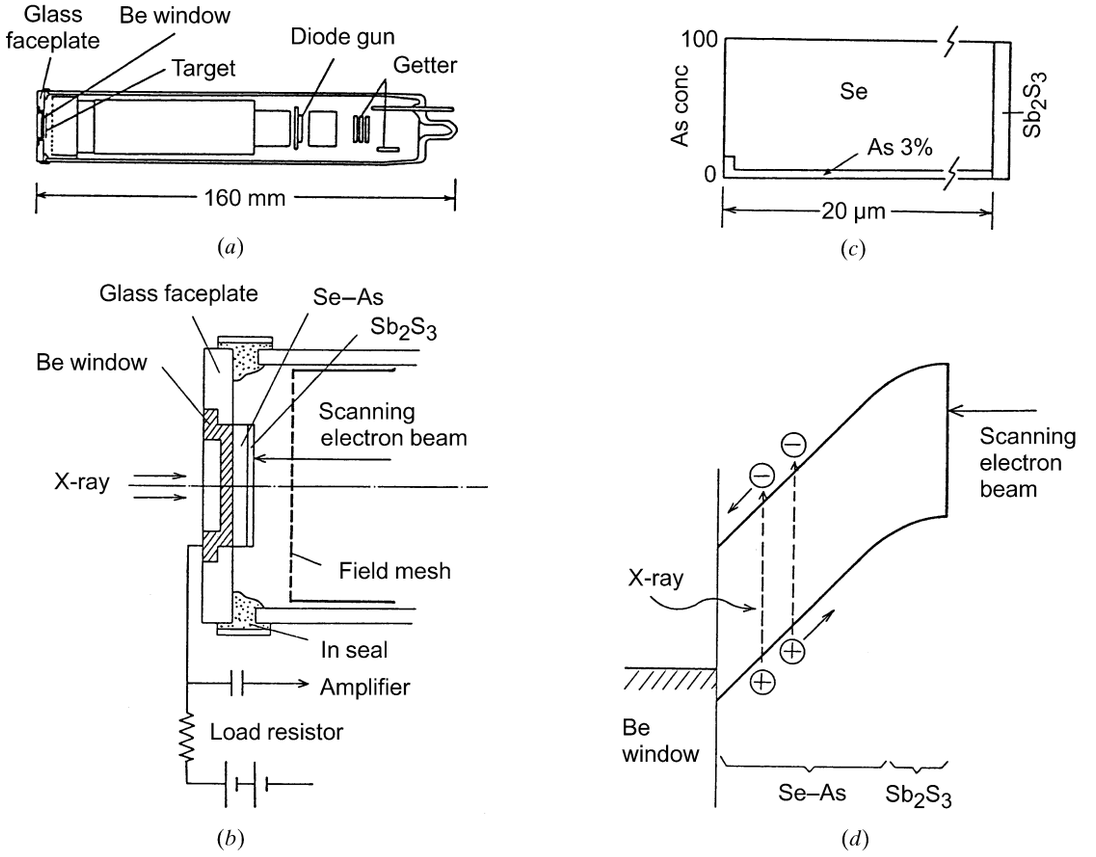

Fig. 7.1.7.1. Schematic illustration of an X-ray sensing Saticon camera tube. (*a*) Schematic representation of the tube. (*b*) Structure of the target. (*c*) Concentration (wt%) of As in the target (Se–As photoconductive layer). Since crystalline Se is metallic, As acts to stabilize the amorphous state. (*d*) Potential in the target. A blocking contact is formed between the X-ray window material and the Se–As alloy layer to prevent holes from flowing into the layer. Incident X-rays form electrons and holes in the layer, and the latter migrate toward the scanning-electron-beam side and contribute to the video signal. On the surface of the Se–As layer, Sb_2S_3 was evaporated to form another blocking contact that improves landing characteristics of the electron beam. By applying a high voltage on the layer, the holes are accelerated to produce multiplication (avalanche amplification), resulting in a great increase of the signal current.

In order to recognize the defect image in the perfect region, the signal-to-noise ratio (SNR) R_I of the image must be

$$R_I \equiv (S_d - S_p)/\sigma_p = \delta C(q\nu_p t)^{1/2} \geq \kappa, \qquad (7.1.7.3)$$

where S_d = signal height of the defect image, C = contrast of the defect image, $C = (S_d - S_p)/S_p$; and κ = threshold SNR of 1–5 (Rose, 1948).

Sensitivity is expressed by the intensity required for a certain signal height to the noise height of the imaging system and is proportional to the value of $q\eta_1 \ldots \eta_s$. As is seen from (7.1.7.3), however, the ratio of the signal to the photon noise depends only on the absorption efficiency q. For example, a 100 μm thick silicon-diode array (Rozgonyi, Haszlo & Statile, 1970) and 15 μm thick lead oxide camera tubes (Chikawa, 1974) have similar sensitivities for Mo $K\alpha$ radiation, but $q = 0.15$ and $q = 0.6$, respectively; the former obtains the sensitivity with a higher conversion efficiency ($\eta_1\eta_2 \ldots \eta_s$) of absorbed photon energy and gives a $(0.15/0.6)^{1/2} = 0.5$ times lower SNR.

It is clear from the foregoing discussion that imaging systems should be evaluated by three factors: resolution, integration time for observation, and SNR.

7.1.7.2. *Imaging system*

There are two kinds of imaging system (*e.g.* Green, 1977); one is a direct method in which X-ray input images are converted directly into video signals and the other is an indirect method in which X-ray images are first converted into visible-light images to be observed by the usual electro-optical system. In the latter, phosphor screens are widely used and the visible images can be magnified by a lens. However, the resolution is limited by the thickness of the phosphor screen that is required for a satisfactory absorption efficiency. In contrast, the direct method provides a high resolution.

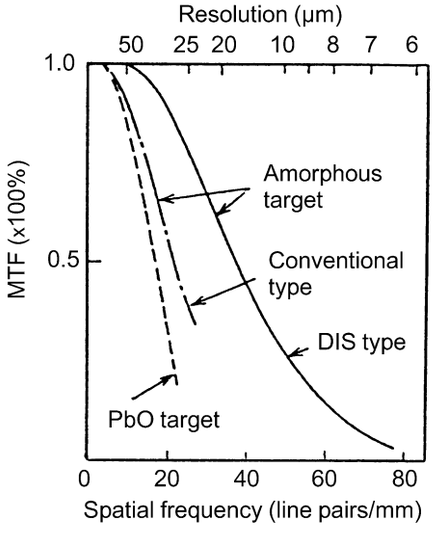

Fig. 7.1.7.2. Square-wave modulation transfer function (MTF) measured for the DIS-type, conventional-type Se–As and PbO camera tubes. This function shows the magnitude of brightness modulation in the output image obtained for an input image with a square-wave intensity distribution and is defined by

$$\mathrm{MTF} = \left(\frac{I_{o\max} - I_{o\min}}{I_{o\max} + I_{o\min}}\right)\left(\frac{I_{i\max} - I_{i\min}}{I_{i\max} + I_{i\min}}\right)^{-1},$$

where $I_{i\max}$ and $I_{i\min}$ are the maximum and minimum intensities of the input image, respectively, and $I_{o\max}$ and $I_{o\min}$ are those of the output. DIS stands for diode-operation impregnated-cathode Saticon.

Various types of indirect method are discussed in Subsections 2.7.5.2 and 7.1.6.5. Here only the direct method will be described in some detail.

A direct method using X-ray TV camera tubes has been used for real-time topography (Chikawa & Matsui, 1994). The construction and operation of an X-ray TV camera tube are similar to those of the conventional video pick-up tube, except for a beryllium window, as shown schematically in Fig. 7.1.7.1. The popular one is a vacuum glass tube which is 15 cm long and 25 mm in diameter. An X-ray sensing photoconductive layer such as Se (McMaster, Photen & Mitchell, 1967), or PbO (Chikawa, 1974) is placed on the inner surface of the window at one end of the tube and is scanned by a narrow electron beam from a cathode on the opposite end to convert image charges on the photoconductive layer into video signals. Therefore, the resolution depends upon the characteristics of the photoconductive layer and the electron-beam size on the layer.

The camera tube with a PbO photoconductive layer has absorption efficiencies of $q = 0.6$ for Mo $K\alpha$ and 0.8 for Cu $K\alpha$, using a PbO layer with a resolution-limited maximum thickness of 15 μm (Chikawa, 1974).

Dislocations in a silicon crystal were observed with the PbO camera tube and a high-power X-ray generator (tube voltage: 60 kV, current: 0.5 A) under the conditions $\nu_p =$

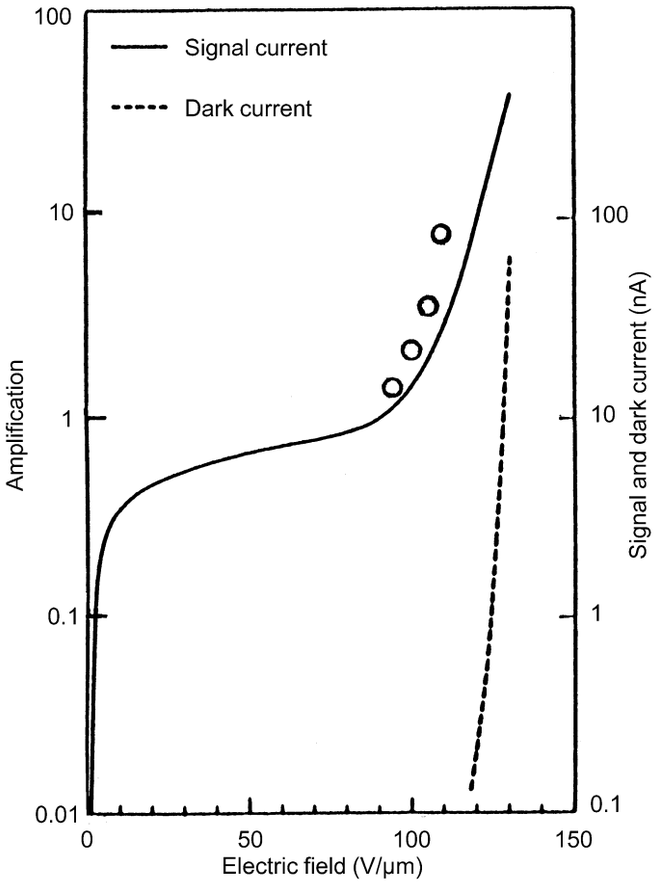

Fig. 7.1.7.3. Typical example showing dependence of the avalanche amplification on the electric field applied on the amorphous photoconductor (HARP). The solid and dashed lines show the amplification of signal current by visible light and dark current, respectively, for a 2 μm thick HARP layer. The right-hand scale shows the current (in nA). The open circles are the data for an 8 μm thick HARP layer by X-ray irradiation. Note that the thicker layer has higher amplifications owing to longer paths for running of holes.

4×10^{11} Mo $K\alpha_1$ photons s^{-1} m^{-2}, $C = 0.5$ and $\delta = 30$ μm (Chikawa, 1974) in (7.1.7.3). In order to improve the resolution further, q must be as high as possible even when ν_p is increased by 10–100 by use of synchrotron radiation, because R_I decreases with improving resolution (decreasing δ). (Note that C is not expected to increase much with improving resolution.) For example, to keep R_I at the same level as the previous case, q should be 0.7, say, for $\nu_p = 10^{13}$ photons s^{-1} m^{-2} and $\delta = 6$ μm. However, resolution and detection efficiency are, in general, mutually exclusive; the resolution of X-ray sensing photoconductive or phosphor materials is determined by the sizes of their grains and their sensitivities decrease with decreasing grain sizes. High resolution, without sacrificing detection efficiency, has been obtained with an amorphous Se–As alloy photoconductive layer, which has the advantage that no degradation of resolution occurs on increasing the layer thickness (Chikawa, Sato, Kawamura, Kuriyama, Yamashita & Goto, 1986). A layer with a thickness of 20 μm has an absorption efficiency of $q = 0.52$ for Mo $K\alpha$. The resolution of these tubes is shown with their modulation transfer functions in Fig. 7.1.7.2. The limiting resolution of 6 μm was obtained by making the scanning electron beam narrower with a diode-type electron gun have a barium-impregnated tungsten cathode (DIS type) (Chikawa, 1999). The Se–As layer shows very low lag characteristics (less than 1% after one frame).

This type of camera tube was developed primarily for TV broadcasting use and named 'Saticon' as the acronym for the components of the photoconductor, Se, As and Te. (Te enhances the sensitivity to red light.)

Such camera tubes have excellent linearity. The output signal current is proportional to the incident X-ray intensity up to 4 μA. The amplifier is always improving in signal-to-noise ratio, and, at present, the noise level of video amplifiers is ~0.2 nA; it is equivalent to an input intensity of $\sim 10^{11}$ Mo $K\alpha$ photons m^{-2} s^{-1} in the US/Japan standard scanning system (30 frames s^{-1}).

Therefore, it is important to increase conversion efficiency ($\eta_1, \eta_2, \ldots, \eta_s$). With increasing voltage applied on the photoconductive layer, the signal current is saturated (in Fig. 7.1.7.1, all the holes produced by an incident photon are collected), and then increases again further by avalanche amplification, as shown in Fig. 7.1.7.3; holes accelerated by a strong electric field cause their multiplication (Sato, Maruyama, Goto, Fujimoto, Shidara, Kawamura, Hirai, Sakai & Chikawa, 1993). It was referred to as 'HARP' (high-gain avalanche-rushing amorphous photoconductor). Together with the signal current, the dark current also increases as shown in Fig. 7.1.7.3. By allowing it to increase to the noise level of the video amplifier, an order of magnitude higher SNR can be achieved. Consequently, individual X-ray photons can be imaged as spots with a size resulting from the point-spread function, unless they are absorbed near the back surface of the photoconductive layer. For X-ray detection, a thick HARP layer should be employed with a very high applied voltage, and stable operation with avalanche amplification was confirmed for a 25 μm thick HARP layer. These pilot tubes were fabricated with a conventional electron gun and had a resolution of about 25 μm.

In general, avalanche amplification results in degradation of spatial resolution and has been used for zero-dimensional detection such as solid-state detectors. To make two-dimensional detection, isolation of each picture element is required. For the HARP, however, no appreciable degradation of resolution due to avalanche amplification was confirmed with a DIS-type tube having an 8 μm thick HARP layer by using visible light through a glass window. X-ray sensitive DIS-type tubes are now commercially available.

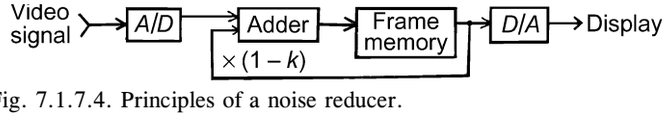

Fig. 7.1.7.4. Principles of a noise reducer.

7.1.7.3. *Image processing*

The resolution δ and integration time t should be selected appropriately according to experimental requirements (Chikawa, 1980). For example, when topographic images of a single dislocation in silicon were observed with $t = 1/30$ s by synchrotron radiation, their contrast and SNR were found to be $C = 0.5$ and $R_I = 20$ for $\delta = 30$ μm, and $C = 1$ and $R_I = 8$ for $\delta = 6$ μm. Since the SNR is desired to be 100, the integration time should be as large as possible unless images of moving objects are degraded. Digital image processing (Heynes, 1977) enables one to adjust the integration time easily. As an example, a noise reducer (McMann, Kreinik, Moore, Kaiser & Rossi, 1978; Rossi, 1978) is shown in Fig. 7.1.7.4. The video signal is sampled and digitized by the A/D converter and the digital video is sent to the adder and thence to the memory. Image information in the memory is continually sent both to the adder through the multiplier for combination with incoming data and to the display through the D/A converter. The weighting of new to old data is made by changing the factor k of the multiplier in the range $0 \le k \le 1$. For $k = 0$, the original input image is displayed. In the range $0 < k < 1$, a sliding summation of successive frames is displayed, and the SNR is improved by a factor of $[(1 + k)/(1 - k)]^{1/2}$. The factor k can be adjusted automatically by detecting the difference between successive frames.

Using a HARP tube, the SNR can be improved without integration of the amplifier noise by image processing, and topographs were displayed with an intensity of $\nu_p \simeq 10^9$ photons s^{-1} m^{-2} by a conventional X-ray generator.

Acquisition of extremely low intensity images, dramatic improvements in SNR *via* frame integration, and isolation and enhancement of selected-contrast ranges are possible by digital image processing (Chikawa & Kuriyama, 1991).

7.1.8. Storage phosphors (By Y. Amemiya and J. Chikawa)

A storage phosphor, called an 'imaging plate', is a two-dimensional detector having a high detective quantum efficiency (DQE) and a large dynamic range. It was developed in the early 1980's for diagnostic radiography (Sonoda, Takano, Miyahara & Kato, 1983; Kato, Miyahara & Takano, 1985). The performance characteristics of the imaging plate was quantitatively evaluated in the mid 1980's (Miyahara, Takahashi, Amemiya, Kamiya & Satow, 1986) and it was proved to be very useful also for X-ray diffraction experiments (Amemiya, Wakabayashi, Tanaka, Ueno & Miyahara, 1987; Amemiya & Miyahara, 1988). The imaging plate has replaced conventional X-ray film in many X-ray diffraction experiments.

The imaging plate (IP) is a flexible plastic plate that is coated with bunches of very small crystals (grain size about 5 μm) of photo-stimulable phosphor [previously BaFBr:Eu^{2+}, recently BaF(Br,I):Eu^{2+}] by using an organic binder. The photo-stimulable phosphor is capable of storing a fraction of the absorbed X-ray energy. When later stimulated by visible light, it emits photo-stimulated luminescence (PSL), the intensity of which is proportional to the absorbed X-ray intensity.